



# Direction-tunable enhanced emission from a subwavelength metallic double-nanoslit structure

XIAOHONG SONG,<sup>1</sup> NINI WANG,<sup>1</sup> MING YAN,<sup>1</sup> CHENG LIN,<sup>1</sup> JENS FÖRSTNER,<sup>2</sup> AND WEIFENG YANG,<sup>1,\*</sup>

<sup>1</sup>Department of Physics, College of Science, Shantou University, Shantou, Guangdong 515063, China

<sup>2</sup>Department of Electrical Engineering, Paderborn University, Warburger Str. 100, 33098, Paderborn, Germany

\*wfyang@stu.edu.cn

**Abstract:** Controlling light emission out of subwavelength nanoslit/aperture structures is of great importance for highly integrated photonic circuits. Here we propose a new method to achieve direction-tunable emission based on a compact metallic microcavity with double nanoslits. Our method combines the principles of Young's interference and surface plasmon polaritons interference. We show that the direction of the far-field beam can be controlled over a wide range of angles by manipulating the frequency and relative phase of light arriving at the two slits, which holds promise for applications in the ultracompact optoelectronic devices.

©2017 Optical Society of America

OCIS codes: (240.6680) Surface plasmons; (260.3910) Metal optics.

## References and links

1. H. A. Bethe, "Theory of diffraction by small holes," *Phys. Rev.* **66**(7-8), 163–182 (1944).
2. T. W. Ebbesen, H. J. Lezec, H. F. Ghaemi, T. Thio, and P. A. Wolff, "Extraordinary optical transmission through sub-wavelength hole arrays," *Nature* **391**(6668), 667–669 (1998).
3. D. E. Grupp, H. J. Lezec, T. W. Ebbesen, K. M. Pellerin, and T. Thio, "Crucial role of metal surface in enhanced transmission through subwavelength apertures," *Appl. Phys. Lett.* **77**(11), 1569–1571 (2000).
4. W. L. Barnes, A. Dereux, and T. W. Ebbesen, "Surface plasmon subwavelength optics," *Nature* **424**(6950), 824–830 (2003).
5. C. Genet and T. W. Ebbesen, "Light in tiny holes," *Nature* **445**(7123), 39–46 (2007).
6. H. Shi, C. Wang, C. Du, X. Luo, X. Dong, and H. Gao, "Beam manipulating by metallic nano-slits with variant widths," *Opt. Express* **13**(18), 6815–6820 (2005).
7. W. Wang, D. Zhao, Y. Chen, H. Gong, X. Chen, S. Dai, Y. Yang, Q. Li, and M. Qiu, "Grating-assisted enhanced optical transmission through a seamless gold film," *Opt. Express* **22**(5), 5416–5421 (2014).
8. H. J. Lezec, A. Degiron, E. Devaux, R. A. Linke, L. Martín-Moreno, F. J. García-Vidal, and T. W. Ebbesen, "Beaming light from a subwavelength aperture," *Science* **297**(5582), 820–822 (2002).
9. W.-J. Lee, J.-B. You, K. Kwon, B. Park, and K. Yu, "Direction-selective emission with small angular divergence from a subwavelength aperture using radiative waveguide modes," *Phys. Rev. B* **87**(12), 125108 (2013).
10. L. Martín-Moreno, F. J. García-Vidal, H. J. Lezec, A. Degiron, and T. W. Ebbesen, "Theory of highly directional emission from a single subwavelength aperture surrounded by surface corrugations," *Phys. Rev. Lett.* **90**(16), 167401 (2003).
11. P. Kramper, M. Agio, C. M. Soukoulis, A. Birner, F. Müller, R. B. Wehrspohn, U. Gösele, and V. Sandoghdar, "Highly directional emission from photonic crystal waveguides of subwavelength width," *Phys. Rev. Lett.* **92**(11), 113903 (2004).
12. S. Kim, H. Kim, Y. Lim, and B. Lee, "Off-axis directional beaming of optical field diffracted by a single subwavelength metal slit with asymmetric dielectric surface gratings," *Appl. Phys. Lett.* **90**(5), 051113 (2007).
13. F. Hao, R. Wang, and J. Wang, "A design methodology for directional beaming control by metal slit grooves structure," *J. Opt.* **13**(1), 015002 (2011).
14. W. Dai and C. M. Soukoulis, "Control of beaming angles via a subwavelength metallic slit surrounded by grooves," *Phys. Rev. B* **82**(4), 045427 (2010).
15. Y. Lee, K. Hoshino, A. Alù, and X. J. Zhang, "Efficient directional beaming from small apertures using surface-plasmon diffraction gratings," *Appl. Phys. Lett.* **101**(4), 041102 (2012).
16. E. Y. Song, H. Kim, W. Y. Choi, and B. Lee, "Active directional beaming by mechanical actuation of double-sided plasmonic surface gratings," *Opt. Lett.* **38**(19), 3827–3829 (2013).
17. Y. Lee, K. Hoshino, A. Alù, and X. J. Zhang, "Tunable directive radiation of surface-plasmon diffraction gratings," *Opt. Express* **21**(3), 2748–2756 (2013).

18. K. Kim, S.-Y. Lee, H. Yun, J.-B. Park, and B. Lee, "Switchable beaming from a nanoslit with metallic gratings controlled by the phase difference between incident beams," *Opt. Express* **22**(5), 5465–5473 (2014).
19. Q. Min and R. Gordon, "Surface plasmon microcavity for resonant transmission through a slit in a gold film," *Opt. Express* **16**(13), 9708–9713 (2008).
20. J. Chen, Z. Li, S. Yue, J. Xiao, and Q. Gong, "Plasmon-induced transparency in asymmetric T-shape single slit," *Nano Lett.* **12**(5), 2494–2498 (2012).
21. A. Haddadpour and G. Veronis, "Microcavity enhanced directional transmission through a subwavelength plasmonic slit," *Opt. Express* **23**(5), 5789–5799 (2015).
22. J. Liu, L. Wang, B. Sun, H. Li, and X. Zhai, "Enhanced optical transmission through a nano-slit based on a dipole source and an annular nano-cavity," *Opt. Laser Technol.* **69**, 71–76 (2015).
23. W. Yao, S. Liu, H. Liao, Z. Li, C. Sun, J. Chen, and Q. Gong, "Efficient Directional Excitation of Surface Plasmons by a Single-Element Nanoantenna," *Nano Lett.* **15**(5), 3115–3121 (2015).
24. X. Zhang, Z. Li, J. Chen, S. Yue, and Q. Gong, "A dichroic surface-plasmon-polariton splitter based on an asymmetric T-shape nanoslit," *Opt. Express* **21**(12), 14548–14554 (2013).
25. H. F. Schouten, N. Kuzmin, G. Dubois, T. D. Visser, G. Gbur, P. F. A. Alkemade, H. Blok, G. W. Hooft, D. Lenstra, and E. R. Eliel, "Plasmon-assisted two-slit transmission: Young's experiment revisited," *Phys. Rev. Lett.* **94**(5), 053901 (2005).
26. H. Shi, X. Luo, and C. Du, "Young's interference of double metallic nanoslit with different widths," *Opt. Express* **15**(18), 11321–11327 (2007).
27. H. Gai, J. Wang, and Q. Tian, "Modified Debye model parameters of metals applicable for broadband calculations," *Appl. Opt.* **46**(12), 2229–2233 (2007).
28. J. Weiner, "The physics of light transmission through subwavelength apertures and aperture arrays," *Rep. Prog. Phys.* **72**(6), 064401 (2009).
29. T. Xu, L. Fang, B. Zeng, Y. Liu, C. Wang, Q. Feng, and X. Luo, "Subwavelength nanolithography based on unidirectional excitation of surface plasmons," *J. Opt. A* **11**(8), 085003 (2009).
30. T. Xu, Y. Zhao, D. Gan, C. Wang, C. Du, and X. Luo, "Directional excitation of surface plasmons with subwavelength slits," *Appl. Phys. Lett.* **92**(10), 101501 (2008).
31. X. Li, Q. Tan, B. Bai, and G. Jin, "Experimental demonstration of tunable directional excitation of surface plasmon polaritons with a subwavelength metallic double slit," *Appl. Phys. Lett.* **98**(25), 251109 (2011).
32. N. Yao, M. Pu, C. Hu, Z. Lai, Z. Zhao, and X. Luo, "Dynamical modulating the directional excitation of surface plasmons sources," *Optik (Stuttg.)* **123**(16), 1465–1468 (2012).
33. J. Chen, Z. Li, M. Lei, S. Yue, J. Xiao, and Q. Gong, "Broadband unidirectional generation of surface plasmon polaritons with dielectric-film-coated asymmetric single-slit," *Opt. Express* **19**(27), 26463–26469 (2011).

## 1. Introduction

According to the diffraction theory, light passing through a subwavelength aperture would be very weak and diffracted in all directions [1]. The diffraction problem also greatly limits integration and miniaturization of conventional optical components. Over the past few decades, advances have allowed metals to be structured and characterized on the nanometer scale, as a result, great efforts have been made to overcome the diffraction limitation with the help of surface plasmon polaritons (SPPs) on metallic surfaces [2–17]. The pioneering work of unusually high transmission through subwavelength periodic hole arrays in metal films was reported by Ebbesen et al. [2]. It was found that the enhanced transmission is induced by the resonant excitation of surface plasmon waves supported by the periodic hole array structure. Several years later, Lezec et al. further reported that a metallic subwavelength slit surrounded by a periodic array of corrugation/grooves that supports the propagation of SPPs cannot only get more light through such structures but also to channel it in a well-defined direction with low divergence [8]. These discoveries have stimulated a large amount of researches in theory and experiment towards further improving beaming characteristics, especially achieving steerable off-axis beaming [9–18]. Up to now, most of the methods proposed for directional beaming are based on subwavelength metal nanoslits with dielectric surface gratings, where the periodic grating structure properties, such as the asymmetry, the period, the depth of the corrugations, and so on, need to be carefully designed for optimal beaming performance [10–18].

Compared with the nanoslit with surrounding periodic grating structures, which are large and difficult to downscale, the unit-cell structures have attracted lots of attention recently since they are much compact and easy to be integrated [19–24]. It has been demonstrated experimentally that a compact surface plasmon microcavity created by trench milling in a gold

film can be used to enhance the transmission of light through a slit [19]. The microcavities can increase the reflectivity at both sides of the trench side-walls, and therefore induce the resonant transmission enhancement. Subsequently, an enhanced transmission revealing an electromagnetically induced transparency (EIT) like optical response has been experimentally demonstrated in a dielectric-film-coated asymmetric microcavity with a slit [20]. Recently, it has been further shown that a compact structure, consisting of multiple optical microcavities at both the entrance and exit sides of a subwavelength plasmonic slit, can lead to greatly enhanced directional transmission through the slit [21]. However, to our knowledge, tunable directive transmission based on unit-cell compact microcavity structures have not yet been reported so far.

In this paper, we propose to utilize a compact dielectric-film-coated metallic microcavity with double-slit to realize the direction-tunable enhanced emission. This structure not only preserves the advantage of SPP microcavity in enhanced transmission, but also makes full use of Young's interference effect of double slits. In the classic double-slit experiment, it has been well known that the position of the interference fringes will be shifted when changing the wavelength ( $\lambda$ ) and the relative phase difference ( $\varphi$ ) of the incident light arriving at the two slits. In metallic double nanoslits, the wavelength and the relative phase difference of the incident light arriving at the two slits can also influence the propagation of the excited SPPs and their coupling to the directly transmitted light from the two slits. Thus by properly tuning the wavelength and relative phase of the incident light arriving at the double slits, the beam angles can be controlled to an arbitrary value over a large range while keeping the structure and material parameters unchanged.

## 2. Simulations and results

Figure 1 shows the schematic of the proposed SPPs microcavity with metallic double-nanoslit structure. The two subwavelength slits (width of  $s = 200\text{nm}$ ) separated by  $d = 600\text{nm}$  are in immediate contact with two steps respectively with widths  $w = 1100\text{nm}$  in the gold film. The thickness of the gold film is  $a = 250\text{nm}$ . The depth of the microcavity, i.e., the height of the metallic steps is  $h = 150\text{nm}$ . It should be noted that though the reflection coefficient will be increased with increasing the height of the metallic walls, the high walls can also induce multiple reflections of SPPs which might decrease the transmittance [20,24]. Unlike the two-slit structures that have been used to study the optical transmission where the slits are separated by many optical wavelengths [25,26], the short slit interval adopted here ensures that the two-slit interference fringes of transmitted light can emit into different directions, moreover, the number of interference fringes is few. The whole structure is coated with a dielectric film of a refractive index of  $n_d = 1.5$  and thickness of  $b = 160\text{nm}$ . The dielectric film makes the SPP field confinement much better [20]. The wave vector of the SPPs on the gold-dielectric interface is given by  $k_{spp} = (2\pi/\lambda_0)\sqrt{\epsilon_m \epsilon_d / (\epsilon_m + \epsilon_d)}$ , where  $\epsilon_m$  and  $\epsilon_d$  are the permittivities of the dielectric and the gold, respectively. Above (several micrometers) the exit of structure, a semi-circle detection port was placed to collect the transmitted far-field light. The far-field angle dependent intensity distribution can be obtained from the time integral of the Poynting vector averaged over the detection port.

Numerical simulations were performed by the Finite-Difference Time-Domain (FDTD) method, using commercial software Remcom XFDTD. According to modified Debye-Drude model [27], the frequency-dependent complex relative permittivity of the gold is defined as:

$$\epsilon(\omega) = \epsilon_\infty + \left( \frac{\epsilon_s - \epsilon_\infty}{1 + i\omega\tau} \right) + \left( \frac{\sigma}{i\omega\epsilon_0} \right), \quad (1)$$

where  $\epsilon_\infty=11.575$  means the infinite-frequency relative permittivity;  $\epsilon_s=-15.789$  is the zero-frequency relative permittivity (static relative permittivity);  $\tau = 8.71 \times 10^{-15} s$  is the relaxation time;  $\sigma=1.6062 \times 10^7 S/m$  is the conductivity;  $\epsilon_0$  is the permittivity of free space.

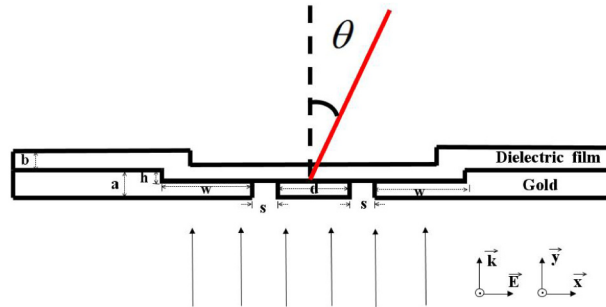


Fig. 1. Schematic and geometry parameters of the proposed double-slit structure for direction-tunable beaming.

In Fig. 2, we present the simulated transmission distribution for three cases with different initial conditions of incident lights. The color map shows the near-field  $H_y$  distribution patterns, while the black dash lines show the corresponding angle dependent far-field intensity distribution, from which essential radiation characteristics like the beam divergence can be deduced. To show clearly the influence of the SPPs on the diffraction field distributions, for each group of parameters, the upper panel shows the cases of light propagation through pure dielectric double-slit structure where no SPPs is excited with other structure parameters are same with those of metal double-slits, while the lower panel shows the case of the metallic double-slit structure as shown in Fig. 1.

It can be seen that when  $\lambda = 750\text{nm}$ ,  $\phi = 0$  in metallic double-slit structure (see Fig. 2(c)), only the 0st order diffraction fringe is enhanced in the case of metallic double-slit structure, the bright fringe is along the perpendicular bisector. The angle dependent far-field intensity distribution shows that only one peak appears at the center, i.e., 0 degree (see Fig. 2(d)). For comparison, we can see that in the pure dielectric double-slit structure without SPPs (see Figs. 2(a) and 2(b)), most of the diffracted light bends away from the normal direction and propagates along the surface, see Fig. 2(a), which is usually called evanescent wave. Only a small part of propagating wave can pass through the slits as propagating light [28]. Above the exit of pure dielectric double-slit structure in air ( $y > 0.5\mu\text{m}$ ), quite weak Young's double slit interference pattern of far-field diffraction light. double-slit diffraction patterns can be discerned: in the normalized far-field angle distribution (see Fig. 2(b)), there are three peaks, one main zero order diffraction peak along  $0^\circ$ , and two  $\pm 1$  order diffraction peaks at about  $\theta = \pm 58.3^\circ$ .

For the proposed metallic double-slit, SPPs will be generated at the exit aperture of each slit and propagate along the bottom of the grooves. The generated SPPs can be reflected back by the walls of the microcavity and then be scattered by the nanoslits and interference with the directly transmitted light [20]. At constructive interference, the transmitted far field in air would be enhanced, otherwise it would be suppressed. By comparing the cases with and without the SPPs, one can see clearly the effects of such interference effects. It can be seen that the  $\pm 1$ st order diffraction fringes in the metallic double-slit microcavity are suppressed and the zeroth order fringe is greatly enhanced. Moreover, the width of the zeroth order fringe becomes much narrower due to the destructive interference between the SPPs and the directly transmitted light, which means that one can get much better directional emission of the transmitted light.

It is known that both the phase of the directly transmitted light and the phase of the generated SPPs depend sensitively on the wavelength  $\lambda$  and the initial phase difference  $\varphi$  of incident light arriving at the two slits [29–32]. In the pure dielectric double-slit structure, changing the parameters of the incident light cannot enhance the propagating light transmitted into air. As we can see in Figs. 2(e) and 2(i), the evanescent wave still dominates the transmitted light. The light propagating into air is all quite weak, but the interference between the directly transmitted light from the two slits induces different interference pattern. For  $\lambda = 850\text{nm}$ ,  $\varphi = 90^\circ$ , the weak diffraction fringes of different orders have comparable intensities, it can be seen in the normalized far-field angle distribution, that there are two peaks, which means that the weak diffraction light is emitted into two directions. Perfect mirror symmetry occurs between  $\varphi = 90^\circ$  and  $\varphi = -90^\circ$  with same  $\lambda$  (see Figs. 2(e), 2(i) and 2(f), 2(j)).

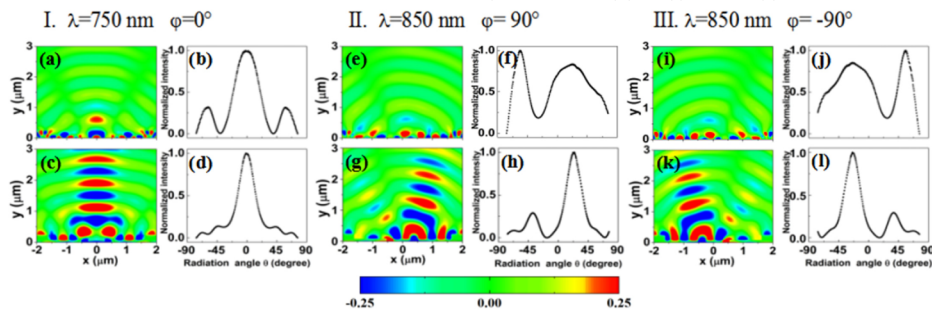


Fig. 2. The simulated transmission distribution for three groups of incident light parameters. Group I, (a)-(d):  $\lambda = 750\text{nm}$ ,  $\varphi = 0^\circ$ ; Group II, (e)-(h):  $\lambda = 850\text{nm}$ ,  $\varphi = 90^\circ$ ; Group III, (i)-(l):  $\lambda = 850\text{nm}$ ,  $\varphi = -90^\circ$ . In each group of parameters, the upper panel shows the case of light propagation through pure dielectric double-slit structure where no SPP is excited while other structure parameters are same with those of metal double-slits. The lower panel shows the case of the metallic double-slit structure as shown in Fig. 1. The color maps show the near-field  $H_y$  distribution patterns. The black dash lines show the corresponding normalized angle dependent far-field intensity distribution.

Contrary to the pure dielectric double-slit structure, in the metallic double-slit structure, changing the parameters of the incident light not only alters the interference pattern of the directly transmitted light, but also the phase of the SPPs. Previous investigations have demonstrated that the SPPs wave generated at each slit can interfere with each other, which can induce the directional propagation of SPPs if the SPPs interfere constructively along one direction while destructively along the opposite direction [29–32]. As can be seen in Fig. 2(g), when  $\lambda = 850\text{nm}$ ,  $\varphi = 90^\circ$ , the SPPs propagating on the right side of the surface are much stronger than those on the left side. This will further influences the interference between the SPPs and the directly transmitted light, making substantial diffraction light are emitted into air along  $\theta = 24.3^\circ$ . From the normalized far-field angle distribution we can see that the oblique beaming has only one main peak whose width is much narrower than that in the pure dielectric double-slit structure. At  $\theta = -38.3^\circ$ , there is also a small peak, however its intensity is much weaker than the one along  $\theta = 24.3^\circ$ , the intensity ratio between these two peaks is approximately 1:4. When  $\lambda = 850\text{nm}$ ,  $\varphi = -90^\circ$ , the one peak oblique beaming is mainly pointing to  $\theta = -24.3^\circ$ , which is mirror symmetric with that of  $\varphi = 90^\circ$ . All these suggest that SPPs propagating along the metal interface lie at the heart of the observed directional emission.

To show clearly how the wavelength and the phase difference of incident light arriving at the two slits influence the transmitted light, we present in Fig. 3 two groups of simulation results, in each group, we fixed a wavelength, but changed the phase difference  $\varphi$ . Since simulation results with  $-\varphi$  show mirror symmetry with  $\varphi$ , we only changed  $\varphi$  from  $0^\circ$  to  $180^\circ$ . It can be seen that for  $\lambda = 700\text{nm}$ , when  $\varphi = 0^\circ$ , there is only one main peak along  $\theta = 0^\circ$ . When  $\varphi$

$\varphi = 45^\circ$ , the peak position is shift to  $\theta = 8.3^\circ$ , moreover, the width of the peak becomes much narrower; When  $\varphi = 90^\circ$ , the peak further slightly shifted to higher emission angle  $\theta = 12.6^\circ$ , but at the same time, the intensity of the satellite peak become larger. Further increased  $\varphi$ , there will be obvious two peaks, which means that the transmitted light emitted into two difference directions. Moreover, the widths of both peaks are wider, which means the directionality becomes worse. From these five simulation results, we can see that good directionality, i.e., small full width at half maximum (FWHM) and large contrast ratio of the different peaks, can be obtained with  $\lambda = 700\text{nm}$ ,  $\varphi = 45^\circ$ , and the emission angle is  $\theta = 8.3^\circ$ . While for  $\lambda = 850\text{nm}$ , cases are much different. It can be seen in this case for  $\varphi = 0^\circ$ , there is a dip at emission angle  $\theta = 0^\circ$ , which means that the bright fringe does not appear at the perpendicular bisector of the double-slit. This phenomenon would never occur in classic dielectric double-slit interference, but can occur in metal double-slit structure, which is caused by the interference between the SPPs and the directly transmitted light along  $\theta = 0^\circ$ . Among these five simulations, good directionality can be achieved with  $\lambda = 850\text{nm}$ ,  $\varphi = 90^\circ$ , in this case, the emission angle is slightly larger, i.e.,  $\theta = 24.3^\circ$ .

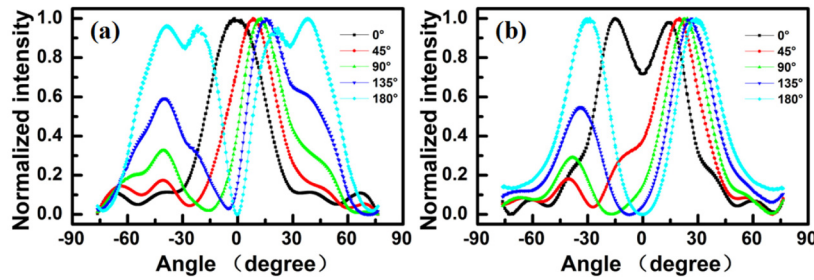


Fig. 3. The simulated transmission distributions for various phase differences  $\varphi$  with fixed wavelength. (a)  $\lambda = 700\text{nm}$ ; (b)  $\lambda = 850\text{nm}$ .

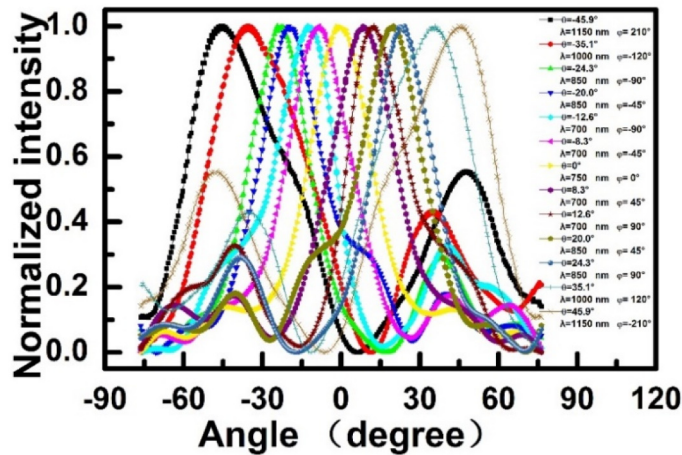


Fig. 4. The normalized angle dependent far-field divergence for different parameters of incident light.

We then scanned the wavelength and relative phase  $\varphi$  with much smaller scanning step to obtain optimum directional emissions of light through metal double-slit structure. We find that the radiation angle of directional beaming can be steered into an arbitrary value over a very large angle range ( $45^\circ \leq \theta \leq 45^\circ$ ) by changing the relative phase of the incident light arriving at the double slits and the wavelength (see Fig. 4). For  $\theta > 45^\circ$ , the intensity of the secondary peak

will be increased (see the black line in Fig. 4) which will affect the directionality of the transmission.

In the following, we will discuss the experimental feasibility of our proposed method. Firstly, we must point out that similar microcavity structure but with only one slit has been recently demonstrated experimentally to be used to achieve enhanced transmission [20]. However, in that work, the enhanced transmitted light is still emitted to different directions. Here we further extend the structure in Ref [20], to have double slit so that directional beaming of the enhanced transmitted light can be achieved. As a result, the experimental realization of this structure is quite reasonable. Secondly, the role of the dielectric film is to increase the SPP field confinement. It is shown that a thickness of 160 nm dielectric film is enough to tightly confine the SPPs [20, 33]. Here we found that the existence of the dielectric film will greatly benefit the transmittance and directionality of the transmitted light (see Fig. 5). Thirdly, the dynamical modulate the relative phase can be achieved through varying the incident angle, which has been demonstrated to achieve directional excitation of SPPs [31]. Using this method, one can change the wavelength while at the same time vary the phase difference. Embedding Kerr nonlinear media in the subwavelength slit might be another feasible choice [32].

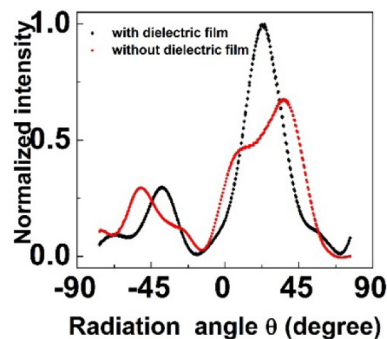


Fig. 5. The simulated transmission distributions with and without dielectric film with  $\lambda = 850\text{nm}$ ,  $\varphi = 90^\circ$ .

### 3. Conclusions

In conclusion, we propose a new method to realize controllable directional transmission in a compact metallic microcavity with double nanoslit. Unlike the conventional metallic double-slit structure which has been used to investigate Young's interference mediated by SPP [25,26] and directional excitation of surface plasmons [23,24,29–33], our structure combines the advantage of surface plasmon (SP) microcavity in enhanced transmission, and the Young's interference effect of double slits. As a result, it is a combined action of different interference processes that induces the controllable directional transmission: the double-slit interference induces different interference/diffraction fringes which pointing to different directions; the interference between the SPPs generated at each slit can enhance or suppress the SPPs along one direction on the metal surface; the interference between the enhanced/suppressed SPPs and the directly transmitted light from the nanoslit enhances/suppresses certain diffraction fringe to achieve directional transmission to only one direction. The proposed structure is quite simple, moreover, one can control the direction of transmission to an arbitrary value over a large range by externally tuning the wavelength and relative phase of the incident light arriving at the double slits. As a result, this proposal may find important applications in integrated devices.

**Funding**

National Natural Science Foundation of China (NSFC) (Grant Nos. 11674209, 11374202 and 11274220); Major Program of Guangdong Natural Science Foundation (Grant No. 2014A030311019); Open Fund of the State Key Laboratory of High Field Laser Physics (SIOM); Innovative Strong School project (2014KTSCX062).

**Acknowledgment**

W. Y. is supported by the “YangFan” Talent Project of Guangdong Province.